ANALYSIS AND DESIGN OF SEISMIC ISOLATION SYSTEMS FOR NUCLEAR STRUCTURES

Y.-N.Huang[1], A.S.Whittaker[2], R.P.Kennedy[3], R.L.Mayes[4]
[1]Dept. of Civil Engineering, National Taiwan University, Taipei, 10617, TAIWAN
[2]The State University of New York at Buffalo, Buffalo, New York, NY 14260, UNITED STATES
[3]RPK Structural Mechanics Consulting, Escondido, California, CA92026, UNITED STATES
[4]Simpson Gumpertz & Heger, Inc., San Francisco, California, CA94105, UNITED STATES
E-mail of corresponding author: ynhuang@ntu.edu.tw

ABSTRACT

ASCE 43-05 presents two performance objectives for the design of nuclear structures: 1) 1% probability of unacceptable performance for 100% Design Basis Earthquake (DBE) shaking, and 2) 10% probability of unacceptable performance for 150% DBE shaking. To develop procedures for the analysis and design of base-isolated nuclear power plants (NPPs) to meet the intent of ASCE 43-05, we performed a series of nonlinear response-history analyses to study the impact of the variability in both earthquake ground motion and mechanical properties of isolation systems on the seismic responses of base-isolated NPPs. Computations were performed for three representative sites (rock and soil sites in the Central and Eastern United States and a rock site in the Western United States), three types of isolators (lead rubber, Friction Pendulum™ and low-damping rubber bearings), and realistic mechanical properties for the isolators. Estimates were made of the ratio of the 99%-ile (90%-ile) response of isolation systems computed using a distribution of spectral demands and distributions of isolator mechanical properties to the median response of isolation systems computed using best-estimate properties and 100% (150%) spectrum-compatible DBE ground motions. Only the results for the soil site in the Central and Eastern United States and LR and FP bearings are presented.

INTRODUCTION

Base isolation has been used to protect buildings, bridges and mission-critical infrastructure from the damaging effect of earthquake shaking [1], [2]. It has been implemented in safety-related nuclear structures in France and South Africa [3]. In the United States, there are no applications of seismic isolation to nuclear structures at the time of this writing although some vendors of Nuclear Steam Supply Systems and power utilities are considering seismic isolation for new build plants.

Two ASCE standards are relevant to the analysis and design of nuclear power plants (NPPs): ASCE 4-98, *Seismic Analysis of Safety-related Nuclear Structures and Commentary* [4] and ASCE 43-05, *Seismic Design Criteria for Structures, Systems and Components in Nuclear Facilities* [5]. Section 1.3 of ASCE 43-05 presents dual performance objectives for nuclear structures: 1) 1% probability of unacceptable performance for 100% Design Basis Earthquake (DBE) shaking, and 2) 10% probability of unacceptable performance for 150% DBE shaking. ASCE Standard 4-98, which includes provisions for the analysis and design of seismic isolation systems, is being updated and the studies reported in Huang et al. [6], [7] provide related information regarding the analysis and design of seismic isolation systems for NPPs to aid in the update of ASCE Standard 4-98. This paper summarizes part of the studies and observations of Huang et al. [6], [7] with a focus on the soil sites in the Central and Eastern United States (CEUS). Information on the studies for rock sites in the CEUS and rock sites in the Western United States is presented in Huang et al. [6], [7].

The goals of the study were to 1) determine the ratio of the 99%-ile estimate of the displacement computed using a distribution of DBE spectral demands and distributions of isolator mechanical properties to the median isolator displacement computed using best-estimate properties and spectrum-compatible DBE shaking; and 2) determine the ratio of the 90%-ile estimate of the displacement computed using a distribution of 150% DBE spectral demands and distributions of isolator mechanical properties to the median isolator displacement computed using best-estimate properties and spectrum-compatible DBE shaking.

Computations were performed for representative rock and soil sites in the Central and Eastern United States (CEUS) and a rock site in the Western United States (WUS). Three types of isolators, namely, low-damping rubber, lead-rubber (LR) and Friction Pendulum (FP) bearings, and realistic mechanical properties for the isolators were used in the analysis. Only the results for the CEUS soil site and LR and FP bearings are presented in this paper. Those for the CEUS soil and WUS rock sites can be found in Huang et al. [6], [7].

The analyses presented in this paper do not consider torsional response of the isolated nuclear structure. If the increment in displacement response due to torsion is a significant percentage of the displacement at the center of mass of the isolated superstructure, the conclusions and recommendations presented below must be used with care. Further, the change in isolator mechanical properties over the course of earthquake shaking was not considered. The dual performance objectives of ASCE 43-05 were established to achieve a mean annual frequency of exceedance (MAFE) less than 10^{-5} for the first onset of significant inelastic deformation (FOSID) of safety-related structures, systems and components in conventional (non-isolated) nuclear facilities. However, the fragility curves for seismic isolation systems are much different from those for typical structural components in NPPs. A study is under way to judge the impact on the MAFE of the unacceptable performance of seismically isolated NPPs if the two performance objectives of ASCE 43-05 are used as the basis for design.

BASE ISOLATION SYSTEMS

Models of Isolation Systems

SAP2000 Nonlinear [8] was used to perform the response-history analysis of models of base-isolated NPPs. Each model was composed of a rigid mass supported by a link element representing the isolation system. Each model had three degrees of freedom: two horizontal and one vertical. The models for each type of the isolation systems used in the analysis are described below:

Lead-rubber (LR) isolation systems were modeled using the “Rubber Isolator” link element in SAP2000. This element has coupled plasticity properties for the two horizontal displacements and linear stiffness properties for the vertical displacement. The plasticity model is similar to that of Figure 1 but the transition between the elastic stiffness and the post-yield stiffness is continuous. To study a wide range of isolation-system properties, 9 best-estimate models were prepared with characteristic strength Q_d equal to 3%, 6% and 9% of the supported weight W , and T_d (the period related to the post-yield stiffness of the isolator K_d through W) equal to 2, 3 and 4 seconds. Parameter T_v (the period related to the vertical stiffness of the isolation system K_v through W) was set to 0.05 second. Only the results for T_d = 3 and 4 seconds and $Q_d = 3\%W$ and $6\%W$ are presented herein and the four models are termed LR_T3Q3, LR_T3Q6, LR_T4Q3 and LR_T4Q6.

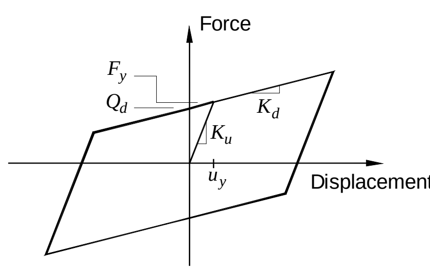

Figure 1: A force-displacement relationship similar to that used in the analysis for this study for LR bearings in the horizontal directions

Friction Pendulum™ (FP) isolators were modeled using the “Friction Isolator” link element that has coupled plasticity properties for the two horizontal directions and a gap element for vertical tensile forces. The coefficient of friction for FP bearings depends on the sliding velocity and is computed in SAP2000 using the following equation [9]:

$$\mu = \mu_{\max} - (\mu_{\max} - \mu_{\min}) \cdot e^{-aV} \tag{1}$$

where μ is the coefficient of sliding friction, varying between $\mu_{\max}$ and $\mu_{\min}$ (for high and very small velocities, respectively), a is a velocity-related parameter, and V is the sliding velocity. Nine best-estimate FP isolation-system models were analyzed in this study with $\mu_{\max}$ equal to 0.03, 0.06 and 0.09 and T_d equal to 2, 3 and 4 seconds but only the results for the three models with $\mu_{\max}$ equal to 0.03 and 0.06 and T_d equal to 3 and 4 seconds are presented. The four models are termed FP_T3Q3, FP_T3Q6, FP_T4Q3 and FP_T4Q6. The yield displacement was set at 1 mm for all FP models. (We note that the recently developed triple concave FP bearing can be configured to produce hysteresis loops similar to that of the LR bearing.)

Variations in properties of isolators

The mechanical properties of LR and FP seismic isolation bearings will tend to vary from the values assumed for design both a) at the time of fabrication due to variability in basic material properties, and b) over the lifespan of the nuclear structure due to aging, contamination, ambient temperature, etc. For LR bearings, the mechanical properties of the lead plug are a function of the confinement provided to the plug and the mechanical properties of the elastomer (rubber). For FP bearings, only the coefficient of sliding friction varies because the second-slope stiffness of the bearing is a function of the radius of the sliding surface, which is constructed to very tight tolerances. Importantly, the variability of the mechanical properties of an assembly of isolators (the isolation *system*) will be smaller than the variability of individual isolators.

To study the impact of the variations in mechanical properties of isolators on the response of base-isolated NPPs, 2 sets of 30 mathematical models were developed for each of the best-estimate models studied herein by modifying the values of key parameters of the best-estimate models. For LR models, Q_d, K_d and K_v were assumed to vary; and for FP models, only $\mu_{\max}$ was assumed to vary. One set of 30 models represents an isolation *system* with *excellent* control on the properties of individual isolators: the probability for the values of the key parameters of the isolation system described above to be within ±10% of the best-estimate values is 95% (Bin F1). The second set represents an isolation *system* with *good* control on the properties of individual isolators: the probability for the values of the key parameters of the isolation system to be within ±20% of the best-estimate values is 95% (Bin F2). We assume the distributions for the values of the key parameters to be normal. As an example, Figure 2 illustrates these distributions in parameters Q_d and K_d for LR isolation systems. Bins F1 and F2 likely address the permissible ranges of mechanical properties of an isolation system for NPP construction. Given that an isolation system consists of a large number of isolators, larger percentage variations in the mechanical properties of individual isolators might be acceptable.

To develop the 2 sets of 30 mathematical models, 2 bins of 30 scale factors were generated, where the factors for Bin F1 (F2) were obtained from a normal distribution with a mean of 1 and a standard deviation of 0.05 (0.1). Figure 3 presents the two normal distributions. For each of these curves in Figure 3, the area under the curve was divided into 30 equal segments; the *midpoint* value in each segment is used to form the factors for Bins F1 and F2.

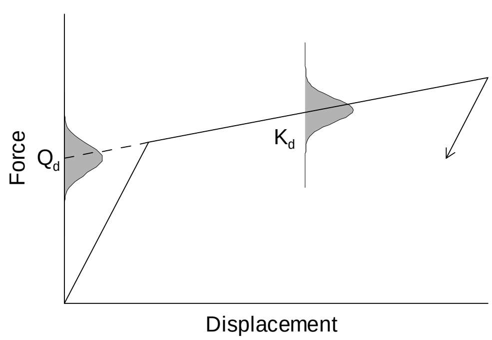

Figure 2: Variations in the mechanical properties of a LR isolation system

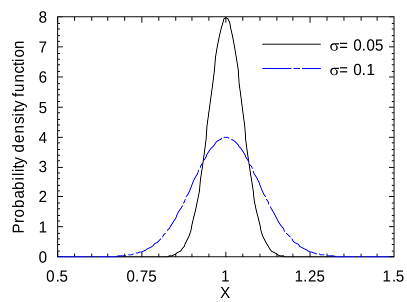

Figure 3: Normal distributions with a mean of 1 and standard deviations of 0.05 and 0.1

The generation of the 2 sets of 30 models for each LR isolation system is presented herein to demonstrate the process. For each best-estimate model of LR_T2Q3, LR_T3Q3 and LR_T4Q3, the values of Q_d, K_d and K_v were scaled by 2 sets of factors: [$\mathrm{F1}_i^{Q_d}$, $\mathrm{F1}_i^{K_d}$, $\mathrm{F1}_i^{K_v}$] and [$\mathrm{F2}_i^{Q_d}$, $\mathrm{F2}_i^{K_d}$, $\mathrm{F2}_i^{K_v}$], where $\mathrm{F1}_i^{Q_d}$, $\mathrm{F1}_i^{K_d}$ and $\mathrm{F1}_i^{K_v}$ ($\mathrm{F2}_i^{Q_d}$, $\mathrm{F2}_i^{K_d}$ and $\mathrm{F2}_i^{K_v}$) are the scale factors for Q_d, K_d and K_v, respectively, determined from the 30 scale factors in Bin F1 (F2) using the Latin Hypercube Sampling procedure [10] and i = 1 through 30. For each value of i, a new model was developed for each case of excellent and good control.

The procedures described above were repeated for the FP isolation system. The developed models were used in the response-history analysis to study the impact of variations in material properties of isolators on the response of base-isolated NPPs.

GROUND MOTIONS FOR A SOIL SITE IN CEUS

Design Basis Earthquake

The site of the Vogtle NPP in Waynesboro, Georgia is a representative soil site for NPPs in CEUS. The horizontal and vertical DBE spectra used in this study for the Vogtle site are presented in Figure 4. The horizontal spectrum of Figure 4 is a uniform-risk spectrum (URS) corresponding to a mean annual frequency of exceedance (MAFE) of 10^{-5} developed by the Southern Nuclear Operating Company for the Vogtle Early Site Permit (ESP) Application [11]. The horizontal DBE spectrum of Figure 4 was scaled by the V/H factors of 0.9 at periods smaller than 0.07 second (15 Hz) and 0.5 at periods greater than 1 second. Interpolation was used to determine the scale factors at periods between 0.07 and 1 second. The technical basis for the V/H scale factors for the spectra of Figure 4 is provided in [11].

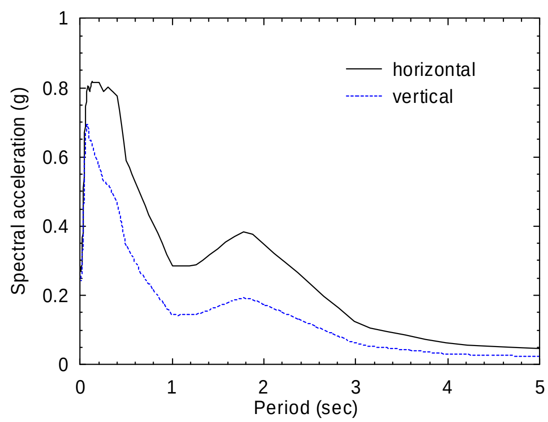

Figure 4: Horizontal and vertical 5% damped DBE spectra for the Votgle NPP site

DBE spectrum-compatible ground motions

Two bins of 30 sets of ground motions were developed for the response-history analysis to study the impact of the variability in earthquake ground motion on the response of base-isolated NPPs. In the first bin, termed DBE spectrum-compatible (DBE-SC) ground motions, both of the two horizontal components of each set of ground motions have 5% damped spectral accelerations similar to that of Figure 4. In the second bin, termed maximum-minimum spectrum-compatible (MM-SC) ground motions, the variability in spectral acceleration along three perpendicular directions is addressed in the scaling of ground motions. The development of these two bins of ground motions are summarized in this and the following subsections, respectively. More information can be found in [6].

Synthetic ground motions were developed in 2 steps. Step 1 involved the use of the deaggregtion data for the Vogtle site and the computer code “Strong Ground Motion Simulation” [12] to generate CEUS-type seed ground motions, which were then spectrally matched to the DBE spectra of Figure 4 in step 2 using the computer code RSPMATCH [13].

Thirty sets of DBE-SC ground motions were developed and each set of ground motions included 2 horizontal components and a vertical component. Panel a of Figure 5 presents a sample DBE-SC acceleration time series and panel b presents the target and achieved spectral accelerations for the time series of panel a. The spectral accelerations for the time series of panel a closely match the target. Panel a of Figure 6 presents the spectral accelerations for horizontal component 1 of all 30 sets of DBE-SC ground motions. Each spectrum of Figure 6a closely matches the target.

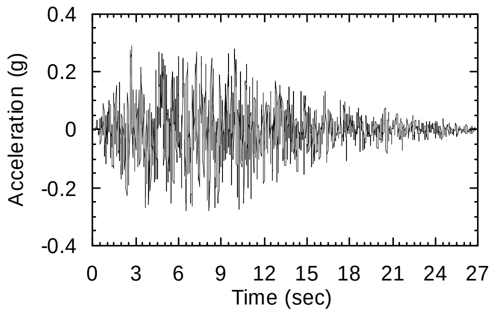

a. time series (horizontal component 1)

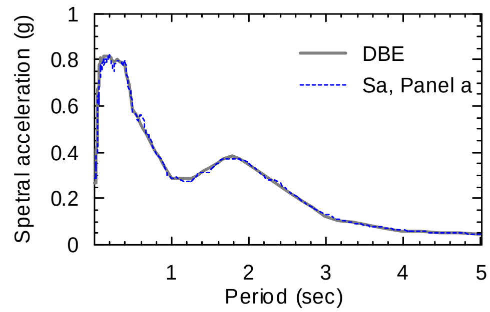

b. spectral acceleration (horizontal component 1)

Figure 5: Sample DBE-SC acceleration time series and the corresponding 5% damped response spectra

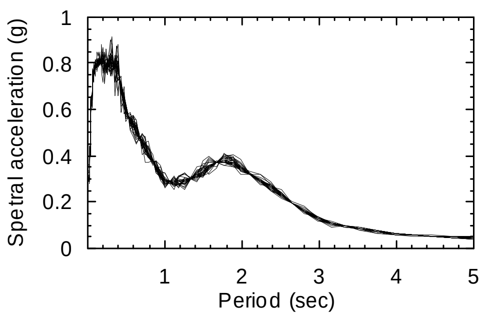

a. spectral acceleration (DBE-SC, horizontal component 1)

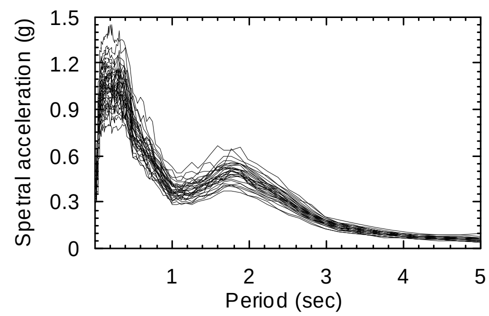

b. spectral acceleration (MM-SC, maximum component)

Figure 6: Five-percent damped response spectra for the DBE-SC and MM-SC ground-motion bins

Maximum-minimum spectra compatible Ground motions

A second set of 30 pairs ground motions, MM-SSC ground motions, were developed by amplitude scaling the 30 sets of DBE-SC ground motions to represent the maximum spectral demand and the demand at the orientation perpendicular to the maximum direction, termed the *minimum* demand. The maximum spectral demand at a given period was defined as the maximum of the spectral accelerations at orientations between 0° to 180° for a pair (the two orthogonal horizontal components) of ground motions [14].

For each set of DBE-SC motions, the 2 horizontal components were amplitude scaled by F_{H_i} and $1/F_{H_i}$, respectively, and the vertical component was amplitude scaled by F_{V_i}. Note that the geometric-mean spectrum for the two scaled horizontal components of a set of ground motions remains the same as the horizontal DBE spectrum of Figure 4. The factors F_{H_i} (F_{V_i}) with $i = 1,30$ were determined using a lognormal distribution with the median of 1.3 (1.0) and logarithmic standard deviation of 0.13 (0.18) using the Latin Hypercube Sampling procedure. Panel b of Figure 6 presents the spectral accelerations for the horizontal component 1 (i.e., the maximum component) of all 30 sets of MM-SC ground motions.

The distribution of F_{H_i} was based on the study of Huang et al. [14], where the median ratio of maximum to geometric-mean (hereafter termed geomean[1]) spectral demands was shown to vary between 1.2 and 1.4 and the logarithmic standard deviation of the ratio varied between 0.11 and 0.13 at periods greater than 2 seconds.

ANALYSIS SETS

Response-history analysis was performed for two intensities of shaking: 1) 100% DBE shaking, using the 60 sets of DBE-SC and MM-SC ground motions, and b) 150% DBE shaking, using the DBE-SC and MM-SC ground motions but with the amplitude of the acceleration time series multiplied by 1.5.

[1] The geomean demand at a given period is computed as the square root of the product of the spectral demands for two orthogonal horizontal ground-motion components.

At each intensity level, 4 sets of analyses were performed for each of the best-estimate models for this study and the corresponding property-varied models. Table 1 summarizes the 4 analysis sets used in this study, denoted G0, M0, M1 and M2.

Set G0 involves response-history analysis of a best-estimate model subjected to 100% and 150% of the 30 sets of DBE-SC ground motions and produces 30 realizations for each of peak bearing displacement and shearing force in the horizontal plane. Here the letter G stands for geomean since the target horizontal DBE spectrum of Figure 4 is a geomean of two horizontal components and the number 0 is used to denote analysis performed using best-estimate models. The data developed from analysis of Set G0 is used to benchmark all other results.

Set M0 is similar to Set G0 but uses 100% and 150% of the 30 sets of MM-SC ground motions. For Set M1 (M2), each of the 30 models associated with a given best-estimate model and mechanical-property scale factors of Bin F1 (F2) is analyzed using the 100% and 150% of 30 sets of MM-SC ground motions. At a given intensity, Sets M1 and M2 each produce 900 realizations (30 sets of ground motions × 30 models) for peak horizontal bearing displacement and transmitted shearing force. Only the results for bearing displacement are presented herein. The results for transmitted shearing force can be found in Huang et al. [6], [7].

Table 1: Analysis sets for this study

Set	Ground motions		Number of models	Quality control	Number of realizations
	Intensity	Bin			
G0	100%,150%	DBE-SC	1	N/A	30
M0	100%,150%	MM-SC	1	N/A	30
M1	100%,150%	MM-SC	30	excellent	900
M2	100%,150%	MM-SC	30	good	900

ANALYSIS RESULTS FOR SOIL SITES IN CEUS

Peak displacement

All realizations in an analysis set are assumed to distribute lognormally with median (θ) and logarithmic standard deviation (β). Table 2 presents θ and β of peak displacement for each case, model and shaking intensity analyzed in this study. The key observations are presented below.

1) For a given model and shaking intensity, the values of θ for M0, M1 and M2 are identical or nearly identical. The median response for analyses accounting for variability in the mechanical properties of the isolation system (i.e., M1 and M2) can be estimated without bias using analysis of a best-estimate model (i.e. M0).
2) The ratio of θ for M0 to G0 ranges between 1.2 and 1.35. If analysis is performed using DBE-SC ground motions (i.e., Set G0), the median displacement should be increased by 20% to 35% to address variability in spectral demands for soil sites in CEUS.
3) The values of β for peak displacement range between 0.1 and 0.3.

Table 2: Medians (θ) and dispersions (β) of peak displacement

Model	100% DBE								150% DBE							
	θ (mm)				β				θ (mm)				β			
	G0	M0	M1	M2	G0	M0	M1	M2	G0	M0	M1	M2	G0	M0	M1	M2
LR_T3Q3	289	349	348	347	0.13	0.18	0.18	0.19	467	558	557	555	0.12	0.15	0.15	0.16
LR_T3Q6	204	264	263	263	0.16	0.24	0.23	0.24	368	456	455	454	0.15	0.21	0.21	0.22
LR_T4Q3	227	274	274	274	0.13	0.20	0.20	0.20	352	425	426	427	0.11	0.18	0.18	0.18
LR_T4Q6	195	238	238	238	0.15	0.23	0.23	0.23	309	373	374	374	0.16	0.23	0.23	0.23
FP_T3Q3	246	303	303	303	0.14	0.20	0.19	0.20	433	523	523	523	0.12	0.15	0.15	0.15
FP_T3Q6	140	190	190	189	0.21	0.30	0.30	0.31	308	391	391	391	0.18	0.25	0.24	0.25
FP_T4Q3	193	240	240	240	0.15	0.22	0.22	0.22	325	403	403	403	0.12	0.19	0.19	0.19
FP_T4Q6	128	168	168	168	0.20	0.29	0.28	0.29	255	319	319	319	0.18	0.26	0.25	0.26

Response scale factors for design

As noted previously, ASCE 43 writes that nuclear structures should achieve two performance goals: 1) less than 1% probability of unacceptable performance for DBE shaking, and 2) less than 10% probability of unacceptable performance for shaking equal to 150% of the DBE ground motion. Factors are presented in Table 3 to scale the median peak displacements for Sets G0 and M0 and 100% DBE shaking to the responses corresponding to 1) 1% probability of exceedance (PE) for Sets M1 and M2 for 100% DBE shaking, and 2) 10% PE for Sets M1 and M2 for 150% DBE shaking.

If response-history analysis is performed using only the DBE-SC ground motions, the factors in the 2nd through 5th columns of Table 3can be used to address the influence of both maximum-demand orientation and the variation in the material properties of isolation systems on responses. The factor corresponding to 1% (10%) PE at 100% (150%) DBE shaking ranges between 1.8 (2.3) and 2.8 (3.9) in Table 3. If response-history analysis is performed using the MM-SC ground motions, the factors in the 6th through 9th columns of Table 3 can be used to address the impact of variation in isolator material properties on response. The factor corresponding to 1% (10%) PE at 100% (150%) DBE shaking ranges between 1.3 (1.2) and 1.8 (1.4) in Table 3.

Table 3: Ratios of displacement for 1% (10%) exceedance probability at 100% (150%) DBE to $\theta_{G0,DBE}$ and $\theta_{M0,DBE}$

Model	$\frac{D_{M1,DBE,99th}}{\theta_{G0,DBE}}$	$\frac{D_{M1,150\%DBE,90th}}{\theta_{G0,DBE}}$	$\frac{D_{M2,DBE,99th}}{\theta_{G0,DBE}}$	$\frac{D_{M2,150\%DBE,90th}}{\theta_{G0,DBE}}$	$\frac{D_{M1,DBE,99th}}{\theta_{M0,DBE}}$	$\frac{D_{M1,150\%DBE,90th}}{\theta_{M0,DBE}}$	$\frac{D_{M2,DBE,99th}}{\theta_{M0,DBE}}$	$\frac{D_{M2,150\%DBE,90th}}{\theta_{M0,DBE}}$
LR_T3Q3	1.83	2.34	1.85	2.37	1.51	1.94	1.53	1.96
LR_T3Q6	2.22	2.91	2.24	2.93	1.72	2.26	1.73	2.27
LR_T4Q3	1.92	2.36	1.93	2.37	1.60	1.96	1.60	1.96
LR_T4Q6	2.06	2.58	2.07	2.58	1.69	2.11	1.69	2.11
FP_T3Q3	1.93	2.57	1.95	2.58	1.57	2.09	1.58	2.09
FP_T3Q6	2.72	3.83	2.80	3.85	2.00	2.82	2.06	2.83
FP_T4Q3	2.09	2.65	2.10	2.66	1.68	2.13	1.68	2.13
FP_T4Q6	2.52	3.44	2.56	3.45	1.93	2.63	1.96	2.64

CLOSING REMARKS

Nonlinear response-history analyses have been performed to study the impact of the variability in both earthquake ground motion and mechanical properties of isolation systems on the seismic responses of base-isolated NPPs. Three types of isolation systems were studied, including LR and single concave FP isolation systems. The analyses were performed for representative rock and soil sites in CEUS and a rock site in WUS but only the results for LR and FP bearings and the selected soil site in the CEUS have been presented here. Key conclusions for the CEUS soil site are summarized below:

1) For a given model, the ratio of median displacement for Set M0 to Set G0 generally ranges between 1.2 and 1.35. The median responses for analyses using DBE-SC ground motions in both horizontal directions should be amplified to address the known variability in spectral demands.
2) The ratios of median responses for Set M1 to Set M0 and those for Set M2 to Set M1 are either equal to or very close to 1 for all cases considered. The median response for analyses accounting for the variability in isolator material properties (i.e., M1 and M2) can be estimated without bias using analysis of a best-estimate model (i.e. M0).
3) The factors to scale the median displacements for Sets G0 and M0 and 100% DBE shaking to the displacements corresponding to 1) 1% PE for Sets M1 and M2 for 100% DBE shaking and 2) 10% PE for Sets M1 and M2 for 150% DBE shaking were studied. The factor for 10% PE and 150% DBE shaking is greater than that for 1% PE and 100% DBE shaking. Analysis of isolator capacity and clearance to surrounding structure can be based on 10% PE for 150% DBE shaking. For Set G0, 10% PE and 150% DBE shaking, the upper bound of the scale factor for LR and FP isolation systems are 2.9 and 3.9, respectively at the representative soil site in CEUS.
4) The difference in the factors to scale the results of analysis of best-estimate models and 100% DBE shaking to 10% PE and 150% DBE shaking for Sets M1 and M2 is negligible.

REFERENCES

[1] Mayes, R. L., Button, M. R. and Jones, D. M. (1998) "Design issues for base isolated bridges: 1997 revised AASHTO code requirements." *Proceedings*, Structural Engineering World Congress, San Francisco, CA.

[2] Naeim, F., and Kelly, J. M. (1999). *Design of seismic isolated structures: from theory to practice*, John Wiley, NY.

[3] Eidinger, J. M., and Kelly, J. M. (1985). "Seismic isolation for nuclear power plants: technical and non-technical aspects in decision making." *Nuclear Engineering and Design*, 84(3), 383-409.

[4] American Society of Civil Engineers (ASCE). (2000). "Seismic analysis of safety-related nuclear structures and commentary." *ASCE 4-98*, ASCE, Reston, VA.

[5] American Society of Civil Engineers (ASCE). (2005). "Seismic design criteria for structures, systems, and components in nuclear facilities." *ASCE/SEI 43-05*, ASCE, Reston, VA.

[6] Huang, Y.-N., Whittaker, A. S., Kennedy, R. P., and Mayes, R. L. (2009). "Assessment of base-isolated nuclear structures for design and beyond-design basis earthquake shaking." *MCEER-09-0008*, Multidisciplinary Center for Earthquake Engineering Research, State University of New York, Buffalo, NY.

[7] Huang, Y.-N., Whittaker, A. S., Kennedy, R. P., and Mayes, R. L. "Beyond-design basis nuclear structures of base isolated nuclear structures." Paper in preparation, *Earthquake Engineering and Structural Dynamics*.

[8] Computers and Structures, Inc. (CSI). (2007). *SAP2000 user's manual – version 11.0*. Berkeley, CA.

[9] Constantinou, M. C., Tsopelas, P., Kasalanati, A., and Wolff, E. D. (1999). "Property modification factors for seismic isolation bearings." *MCEER-99-0012*, Multidisciplinary Center for Earthquake Engineering Research, State University of New York, Buffalo, NY.

[10] Nowak, A. S., and Collins, K. R. (2000). *Reliability of structures*, McGraw-Hill, Boston.

[11] Southern Nuclear Operating Company (SNOC). (2008). *Vogtle Early Site Permit Application*, SNOC. < http://adamswebsearch2.nrc.gov/idmws/ViewDocByAccession.asp?AccessionNumber=ML081020073 >

[12] Halldorsson, B. (2004). <civil.eng.buffalo.edu/engseislab/ products.htm> Engineering Seismology Laboratory, State University of New York, Buffalo, NY.

[13] Abrahamson, N.A. (1998). "Non-stationary spectral matching program RSPMATCH." PG&E, Internal Report.

[14] Huang, Y.-N., Whittaker, A. S., and Luco, N. (2008). "Maximum spectral demands in the near-fault region." *Earthquake Spectra*, 24(1), 319-341.